

# A Hybrid-STATCOM With Wide Compensation Range and Low DC-Link Voltage

Lei Wang, Chi-Seng Lam, *Senior Member, IEEE*, and Man-Chung Wong, *Senior Member, IEEE*

**Abstract**—This paper proposes a hybrid static synchronous compensator (hybrid-STATCOM) in a three-phase power transmission system that has a wide compensation range and low dc-link voltage. Because of these prominent characteristics, the system costs can be greatly reduced. In this paper, the circuit configuration of hybrid-STATCOM is introduced first. Its  $V-I$  characteristic is then analyzed, discussed, and compared with traditional STATCOM and capacitive-coupled STATCOM (C-STATCOM). The system parameter design is then proposed on the basis of consideration of the reactive power compensation range and avoidance of the potential resonance problem. After that, a control strategy for hybrid-STATCOM is proposed to allow operation under different voltage and current conditions, such as unbalanced current, voltage dip, and voltage fault. Finally, simulation and experimental results are provided to verify the wide compensation range and low dc-link voltage characteristics and the good dynamic performance of the proposed hybrid-STATCOM.

**Index Terms**—Capacitive-coupled static synchronous compensator (C-STATCOM), hybrid-STATCOM, low dc-link voltage, STATCOM, wide compensation range.

## I. INTRODUCTION

THE LARGE reactive current in transmission systems is one of the most common power problems, which increases transmission losses and lowers the stability of a power system [1]–[19]. Application of reactive power compensators is one of the solutions for this issue.

Static Var compensators (SVCs) are traditionally used to dynamically compensate reactive currents as the loads vary from time to time. However, SVCs suffer from many problems, such as resonance problems, harmonic current injection, and slow response [2], [3]. To overcome these disadvantages, static synchronous compensators (STATCOMs) and active power filters (APFs) were developed for reactive current compensation with faster response, less harmonic current injection, and better

Manuscript received June 13, 2015; revised October 2, 2015 and November 21, 2015; accepted December 23, 2015. Date of publication February 8, 2016; date of current version May 10, 2016. This work was supported in part by the Macau Science and Technology Development Fund (FDCT) (FDCT 109/2013/A3) and in part by the Research Committee of the University of Macau (MRG012/WMC/2015/FST, MYRG2015-00030-AMSV) (Corresponding author: Chi-Seng Lam.)

L. Wang is with the Department of Electrical and Computer Engineering, Faculty of Science and Technology, University of Macau, Macau 999078, China (e-mail: jordanwanglei@gmail.com).

C.-S. Lam and M.-C. Wong are with the Department of Electrical and Computer Engineering, Faculty of Science and Technology, and the State Key Laboratory of Analog and Mixed Signal VLSI, University of Macau, Macau 999078, China (e-mail: cslam@umac.mo; c.s.lam@ieee.org; mcwong@umac.mo).

Color versions of one or more of the figures in this paper are available online at <http://ieeexplore.ieee.org>.

Digital Object Identifier 10.1109/TIE.2016.2523922

performance [4]–[9]. However, the STATCOMs or APFs usually require multilevel structures in a medium- or high-voltage level transmission system to reduce the high-voltage stress across each power switch and dc-link capacitor, which drives up the initial and operational costs of the system and also increases the control complexity. Later, series-type capacitive-coupled STATCOMs (C-STATCOMs) were proposed to reduce the system dc-link operating voltage requirement [10], and other series-type hybrid structures that consist of different passive power filters (PPFs) in series with STATCOMs or APF structures (PPF-STATCOMs) have been applied to power distribution systems [11]–[16] and traction power systems [17]–[19]. However, C-STATCOMs and other series-type PPF-STATCOMs contain relatively narrow reactive power compensation ranges. When the required compensating reactive power is outside their compensation ranges, their system performances can significantly deteriorate.

To improve the operating performances of the traditional STATCOMs, C-STATCOMs, and other PPF-STATCOMs, many different control techniques have been proposed, such as the instantaneous  $p-q$  theory [4], [10], [11], [17]–[19], the instantaneous  $d-q$  theory [5], [6], [14], the instantaneous  $i_d-i_q$  method [7], negative- and zero-sequence control [8], the back propagation (BP) control method [9], nonlinear control [12], Lyapunov-function-based control [13], instantaneous symmetrical component theory [15], and hybrid voltage and current control [16].

To reduce the current rating of the STATCOMs or APFs, a hybrid combination structure of PPF in parallel with STATCOM (PPF//STATCOM) was proposed in [20] and [21]. However, this hybrid compensator is dedicated for inductive loading operation. When it is applied for capacitive loading compensation, it easily loses its small active inverter rating characteristics. To enlarge the compensation range and keep low current rating characteristic of the APF, Dixon *et al.* [22] proposed another hybrid combination structure of SVC in parallel with APF (SVC//APF) in three-phase distribution systems. In this hybrid structure, the APF is controlled to eliminate the harmonics and compensate for the small amounts of load reactive and unbalanced power left by the SVC. However, if this structure is applied in a medium- or high-voltage-level transmission system, the APF still requires a costly voltage step-down transformer and/or multilevel structure. In addition, these two parallel connected-hybrid-STATCOM structures [15]–[17] may suffer from a resonance problem.

To overcome the shortcomings of different reactive power compensators [1]–[22] for transmission systems, this paper proposes a hybrid-STATCOM that consists of a

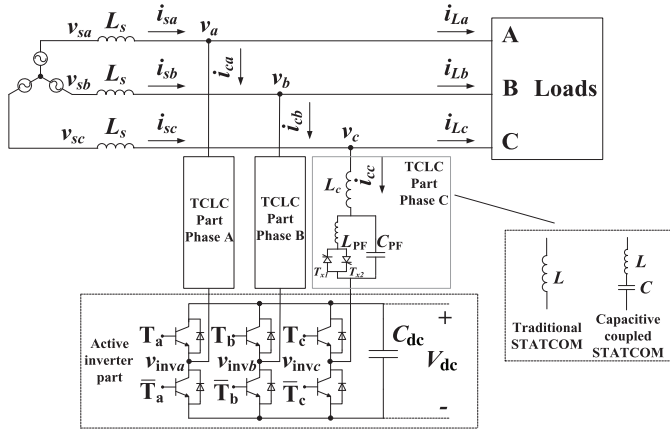


Fig. 1. Circuit configuration of the hybrid-STATCOM.

thyristor-controlled LC (TCLC) part and an active inverter part, as shown in Fig. 1. The TCLC part provides a wide reactive power compensation range and a large voltage drop between the system voltage and the inverter voltage so that the active inverter part can continue to operate at a low dc-link voltage level. The small rating of the active inverter part is used to improve the performances of the TCLC part by absorbing the harmonic currents generated by the TCLC part, avoiding mistuning of the firing angles, and preventing the resonance problem. The contributions of this paper are summarized as follows.

- 1) A hybrid-STATCOM is proposed, with the distinctive characteristics of a much wider compensation range than C-STATCOM [10] and other series-type PPF-STATCOMs [11]–[19] and a much lower dc-link voltage than traditional STATCOM [4]–[9] and other parallel-connected hybrid-STATCOMs [20]–[22].
- 2) Its  $V$ – $I$  characteristic is analyzed to provide a clear view of the advantages of hybrid-STATCOM in comparison with traditional STATCOM and C-STATCOM.
- 3) Its parameter design method is proposed based on consideration of the reactive power compensation range, prevention of the potential resonance problem, and avoidance of mistuning of firing angle.
- 4) A new control strategy for hybrid-STATCOM is proposed to coordinate the TCLC part and the active inverter part for reactive power compensation under different voltage and current conditions, such as unbalanced current, voltage fault, and voltage dip.

The characteristics of different reactive power compensators and the proposed hybrid-STATCOM for the transmission system are compared and summarized in Table I.

In this paper, the system configuration of the proposed hybrid-STATCOM is introduced in Section II. In Section III, the  $V$ – $I$  characteristic of hybrid-STATCOM is proposed in comparison with traditional STATCOM and C-STATCOM. The parameter design and control strategy of the hybrid-STATCOM are then proposed in Sections IV and V. Finally, the simulation (Section VI) and experimental results (Section VII) are provided to prove the wide compensation range and low dc-link voltage characteristics and the dynamic performance of the proposed hybrid-STATCOM.

TABLE I  
CHARACTERISTICS OF DIFFERENT COMPENSATORS FOR TRANSMISSION SYSTEM

	Response time	Resonance problem	DC-link voltage	Compensation range	Cost
SVCs [2]–[3]	Slow	Yes	–	Wide	Low
STATCOMs [4]–[9]	Very Fast	No	High	Wide	High
C-STATCOMs [10]	Fast	No	Low	Narrow	Low
Series-type PPF-STATCOMs [11]–[19]	Fast	No	Low	Narrow	Low
PPF//STATCOM [20], [21]	Fast	Yes	High	Narrow	Medium
SVC//APF [22]	Fast	Yes	High	Wide	High
Hybrid-STATCOM	Fast	No	Low	Wide	Medium

\*Shaded areas indicate an unfavorable characteristic.

## II. CIRCUIT CONFIGURATION OF THE HYBRID-STATCOM

Fig. 1 shows the circuit configuration of hybrid-STATCOM, in which the subscript  $x$  stands for phase  $a, b,$  and  $c$  in the following analysis.  $v_{sx}$  and  $v_x$  are the source and load voltages;  $i_{sx}$ ,  $i_{Lx}$ , and  $i_{cx}$  are the source, load, and compensating currents, respectively.  $L_s$  is the transmission line impedance. The hybrid-STATCOM consists of a TCLC and an active inverter part.

The TCLC part is composed of a coupling inductor  $L_c$ , a parallel capacitor  $C_{PF}$ , and a thyristor-controlled reactor with  $L_{PF}$ . The TCLC part provides a wide and continuous inductive and capacitive reactive power compensation range that is controlled by controlling the firing angles  $\alpha_x$  of the thyristors. The active inverter part is composed of a voltage source inverter with a dc-link capacitor  $C_{dc}$ , and the small rating active inverter part is used to improve the performance of the TCLC part. In addition, the coupling components of the traditional STATCOM and C-STATCOM are also presented in Fig. 1.

Based on the circuit configuration in Fig. 1, the  $V$ – $I$  characteristics of traditional STATCOM, C-STATCOM, and hybrid-STATCOM are compared and discussed.

## III. $V$ – $I$ CHARACTERISTICS OF THE TRADITIONAL STATCOM, C-STATCOM, AND HYBRID-STATCOM

The purpose of the hybrid-STATCOM is to provide the same amount of reactive power as the loadings ( $Q_{Lx}$ ) consumed, but with the opposite polarity ( $Q_{cx} = -Q_{Lx}$ ). The hybrid-STATCOM compensating reactive power  $Q_{cx}$  is the sum of the reactive power  $Q_{TCLC}$  that is provided by the TCLC part and the reactive power  $Q_{invx}$  that is provided by the active inverter part. Therefore, the relationship among  $Q_{Lx}$ ,  $Q_{TCLC}$ , and  $Q_{invx}$  can be expressed as

$$Q_{Lx} = -Q_{cx} = -(Q_{TCLC} + Q_{invx}). \quad (1)$$

The reactive powers can also be expressed in terms of voltages and currents as

$$Q_{Lx} = V_x I_{Lqx} = -(X_{TCLC}(\alpha_x) I_{cq}^2 + V_{invx} I_{cq}) \quad (2)$$

where  $X_{TCLC}(\alpha_x)$  is the coupling impedance of the TCLC part;  $\alpha_x$  is the corresponding firing angle;  $V_x$  and  $V_{invx}$  are the

root-mean-squared (RMS) values of the coupling point and the inverter voltages; and  $I_{Lqx}$  and  $I_{cqx}$  are the RMS value of the load and compensating reactive currents, where  $I_{Lqx} = -I_{cqx}$ . Therefore, (2) can be further simplified as

$$V_{invx} = V_x + X_{TCLC}(\alpha_x)I_{Lqx} \quad (3)$$

where the TCLC part impedance  $X_{TCLC}(\alpha_x)$  can be expressed as

$$\begin{aligned} X_{TCLC}(\alpha_x) &= \frac{X_{TCLC}(\alpha_x)X_{C_{PF}}}{X_{C_{PF}} - X_{TCLC}(\alpha_x)} + X_{L_c} \\ &= \frac{\pi X_{L_{PF}} X_{C_{PF}}}{X_{C_{PF}}(2\pi - 2\alpha_x + \sin 2\alpha_x) - \pi X_{L_{PF}}} + X_{L_c} \end{aligned} \quad (4)$$

where  $X_{L_c}$ ,  $X_{L_{PF}}$ , and  $X_{C_{PF}}$  are the fundamental impedances of  $L_c$ ,  $L_{PF}$ , and  $C_{PF}$ , respectively. In (4), it is shown that the TCLC part impedance is controlled by firing angle  $\alpha_x$ . And the minimum inductive and capacitive impedances (absolute value) of the TCLC part can be obtained by substituting the firing angles  $\alpha_x = 90^\circ$  and  $\alpha_x = 180^\circ$ , respectively. In the following discussion, the minimum value for impedances stands for its absolute value. The minimum inductive ( $X_{ind(min)} > 0$ ) and capacitive ( $X_{Cap(min)} < 0$ ) TCLC part impedances can be expressed as

$$X_{ind(min)}(\alpha_x = 90^\circ) = \frac{X_{L_{PF}} X_{C_{PF}}}{X_{C_{PF}} - X_{L_{PF}}} + X_{L_c} \quad (5)$$

$$X_{Cap(min)}(\alpha_x = 180^\circ) = -X_{C_{PF}} + X_{L_c}. \quad (6)$$

Ideally,  $X_{TCLC}(\alpha_x)$  is controlled to be  $V_x \approx X_{TCLC}(\alpha_x)I_{Lqx}$ , so that the minimum inverter voltage ( $V_{invx} \approx 0$ ) can be obtained as shown in (3). In this case, the switching loss and switching noise can be significantly reduced. A small inverter voltage  $V_{invx(min)}$  is necessary to absorb the harmonic current generated by the TCLC part, to prevent a resonance problem, and to avoid mistuning the firing angles. If the loading capacitive current or inductive current is outside the TCLC part compensating range, the inverter voltage  $V_{invx}$  will be slightly increased to further enlarge the compensation range.

The coupling impedances for traditional STATCOM and C-STATCOM, as shown in Fig. 1, are fixed as  $X_L$  and  $X_C - 1/X_L$ . The relationships among the load voltage  $V_x$ , the inverter voltage  $V_{invx}$ , the load reactive current  $I_{Lqx}$ , and the coupling impedance of traditional STATCOM and C-STATCOM can be expressed as

$$V_{invx} = V_x + X_L I_{Lqx} \quad (7)$$

$$V_{invx} = V_x - \left( X_C - \frac{1}{X_L} \right) I_{Lqx} \quad (8)$$

where  $X_L \gg X_C$ . Based on (3)–(8), the  $V$ – $I$  characteristics of the traditional STATCOM, C-STATCOM, and hybrid-STATCOM can be plotted as shown in Fig. 2.

For traditional STATCOM as shown in Fig. 2(a), the required  $V_{invx}$  is larger than  $V_x$  when the loading is inductive. In contrast, the required  $V_{invx}$  is smaller than  $V_x$  when the loading is

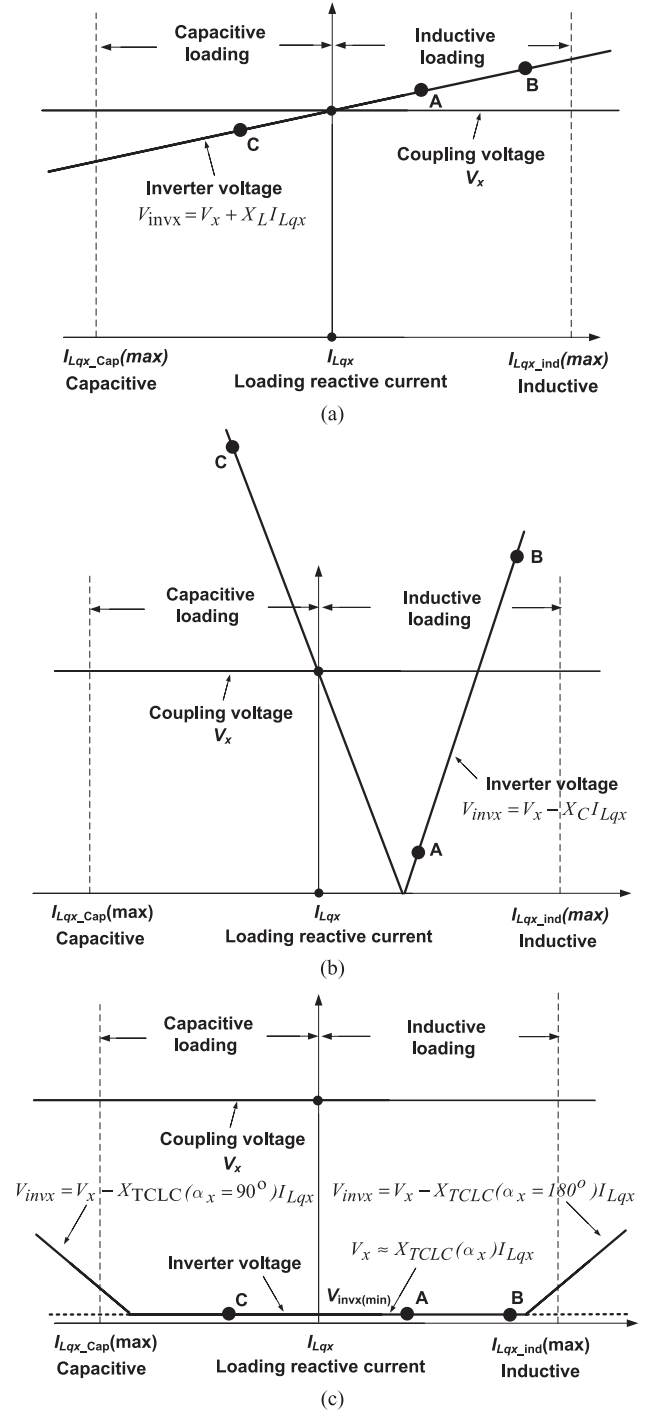


Fig. 2.  $V$ – $I$  characteristic of (a) traditional STATCOM; (b) C-STATCOM; and (c) hybrid-STATCOM.

capacitive. Actually, the required inverter voltage  $V_{invx}$  is close to the coupling voltage  $V_x$ , due to the small value of coupling inductor  $L$  [5]–[8].

For C-STATCOM as shown in Fig. 2(b), it is shown that the required  $V_{invx}$  is lower than  $V_x$  under a small inductive loading range. The required  $V_{invx}$  can be as low as zero when the coupling capacitor can fully compensate for the loading reactive current. In contrast,  $V_{invx}$  is larger than  $V_x$  when the loading is capacitive or outside its small inductive loading range. Therefore, when the loading reactive current is outside

its designed inductive range, the required  $V_{\text{inv}x}$  can be very large.

For the proposed hybrid-STATCOM as shown in Fig. 2(c), the required  $V_{\text{inv}x}$  can be maintained at a low (minimum) level ( $V_{\text{inv}x(\text{min})}$ ) for a large inductive and capacitive reactive current range. Moreover, when the loading reactive current is outside the compensation range of the TCLC part, the  $V_{\text{inv}x}$  will be slightly increased to further enlarge the compensating range. Compared with traditional STATCOM and C-STATCOM, the proposed hybrid-STATCOM has a superior  $V-I$  characteristic of a large compensation range with a low inverter voltage.

In addition, three cases represented by points *A*, *B*, and *C* in Fig. 2 are simulated in Section VI. Based on Fig. 1, the parameter design of hybrid-STATCOM is discussed in the following section.

#### IV. PARAMETER DESIGN OF HYBRID-STATCOM

The proposed TCLC part is a newly proposed SVC structure which designed based on the basis of the consideration of the reactive power compensation range (for  $L_{\text{PF}}$  and  $C_{\text{PF}}$ ) and the prevention of the potential resonance problem (for  $L_c$ ). The active inverter part (dc-link voltage  $V_{\text{dc}}$ ) is designed to avoid mistuning of the firing angle of TCLC part.

##### A. Design of $C_{\text{PF}}$ and $L_{\text{PF}}$

The purpose of the TCLC part is to provide the same amount of compensating reactive power  $Q_{cx, \text{TCLC}}(\alpha_x)$  as the reactive power required by the loads  $Q_{Lx}$  but with the opposite direction. Therefore,  $C_{\text{PF}}$  and  $L_{\text{PF}}$  are designed on the basis of the maximum capacitive and inductive reactive power. The compensating reactive power  $Q_{cx}$  range in term of TCLC impedance  $X_{\text{TCLC}}(\alpha_x)$  can be expressed as

$$Q_{cx, \text{TCLC}}(\alpha_x) = \frac{V_x^2}{X_{\text{TCLC}}(\alpha_x)} \quad (9)$$

where  $V_x$  is the RMS value of the load voltage and  $X_{\text{TCLC}}(\alpha_x)$  is the impedance of the TCLC part, which can be obtained from (4). In (9), when the  $X_{\text{TCLC}}(\alpha_x) = X_{\text{Cap}(\text{min})}(\alpha_x = 180^\circ)$  and  $X_{\text{TCLC}}(\alpha_x) = X_{\text{Ind}(\text{min})}(\alpha_x = 90^\circ)$ , the TCLC part provides the maximum capacitive and inductive compensating reactive power  $Q_{cx(\text{MaxCap})}$  and  $Q_{cx(\text{MaxInd})}$ , respectively,

$$Q_{cx(\text{MaxCap})} = \frac{V_x^2}{X_{\text{Cap}(\text{min})}(\alpha_x = 180^\circ)} = -\frac{V_x^2}{X_{C_{\text{PF}}} - X_{L_c}} \quad (10)$$

$$Q_{cx(\text{MaxInd})} = \frac{V_x^2}{X_{\text{Ind}(\text{min})}(\alpha_x = 90^\circ)} = \frac{V_x^2}{\frac{X_{L_{\text{PF}}} X_{C_{\text{PF}}}}{X_{C_{\text{PF}}} - X_{L_{\text{PF}}}} + X_{L_c}} \quad (11)$$

where the minimum inductive impedance  $X_{\text{Ind}(\text{min})}$  and the capacitive impedance  $X_{\text{Cap}(\text{min})}$  are obtained from (5) and (6), respectively.

To compensate for the load reactive power ( $Q_{cx} = -Q_{Lx}$ ),  $C_{\text{PF}}$  and  $L_{\text{PF}}$  can be deduced on the basis of the loading maximum inductive reactive power  $Q_{Lx(\text{MaxInd})}$

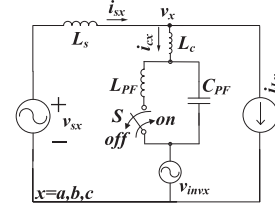


Fig. 3. Simplified single-phase equivalent circuit model of hybrid-STATCOM.

( $= -Q_{cx(\text{MaxCap})}$ ) and capacitive reactive power  $Q_{Lx(\text{MaxCap})}$  ( $= -Q_{cx(\text{MaxInd})}$ ). Therefore, based on (10) and (11), the parallel capacitor  $C_{\text{PF}}$  and inductor  $L_{\text{PF}}$  can be designed as

$$C_{\text{PF}} = \frac{Q_{Lx(\text{MaxInd})}}{\omega^2 Q_{Lx(\text{MaxInd})} L_c + \omega V_x^2} \quad (12)$$

$$L_{\text{PF}} = \frac{V_x^2 + \omega L_c Q_{Lx(\text{MaxCap})}}{-\omega Q_{Lx(\text{MaxCap})} + \omega^3 L_c C_{\text{PF}} Q_{Lx(\text{MaxCap})} + \omega^2 V_x^2 C_{\text{PF}}} \quad (13)$$

where  $\omega$  is the fundamental angular frequency and  $V_x$  is the RMS load voltage.

##### B. Design of $L_c$

For exciting resonance problems, a sufficient level of harmonic source voltages or currents must be present at or near the resonant frequency. Therefore,  $L_c$  can be designed to tune the resonance points to diverge from the dominated harmonic orders  $n_d = 6n \pm 1$ th ( $n = 1, 2, 3$ , etc.) of a three-phase three-wire transmission system to avoid the resonance problem.

The thyristors ( $T_{x1}$  and  $T_{x2}$ ) for each phase of the TCLC part can be considered as a pair of bidirectional switches that generate low-order harmonic currents when the switches change states. The simplified single-phase equivalent circuit model of hybrid-STATCOM is shown in Fig. 3.

Referring to Fig. 3, when switch  $S$  is turned off, the TCLC part can be considered as the  $L_c$  in series with  $C_{\text{PF}}$ , which is called  $LC$ -mode. In contrast, when switch  $S$  is turned on, the TCLC can be considered as the  $L_c$  in series with the combination of  $C_{\text{PF}}$  in parallel with  $L_{\text{PF}}$ , which is called  $LCL$ -mode. From Table IV, the TCLC part harmonic impedances under  $LC$ -mode and  $LCL$ -mode at different harmonic order  $n$  can be plotted in Fig. 4 and expressed as

$$X_{LC, n}(n) = \left| \frac{1 - (n\omega)^2 L_c C_{\text{PF}}}{n\omega C_{\text{PF}}} \right| \quad (14)$$

$$X_{LCL, n}(n) = \left| \frac{n\omega(L_c + L_{\text{PF}}) - (n\omega)^3 L_{\text{PF}} L_c C_{\text{PF}}}{1 - (n\omega)^2 L_{\text{PF}} C_{\text{PF}}} \right| \quad (15)$$

In (14) and (15), there are two series resonance points  $n_1$  at  $X_{LC, n}(n_1) = 0$  and  $n_2$  at  $X_{LCL, n}(n_2) = 0$ , and a parallel resonance point  $n_3$  at  $X_{LCL, n}(n_3) = +\infty$ .  $L_c$  can be designed to tune the resonance points  $n_1$  and  $n_2$  to diverge from the dominated harmonic orders  $n_d = 6n \pm 1$ th ( $n = 1, 2, 3 \dots$ ) or approach the  $3n$ th order in a three-phase three-wire system.

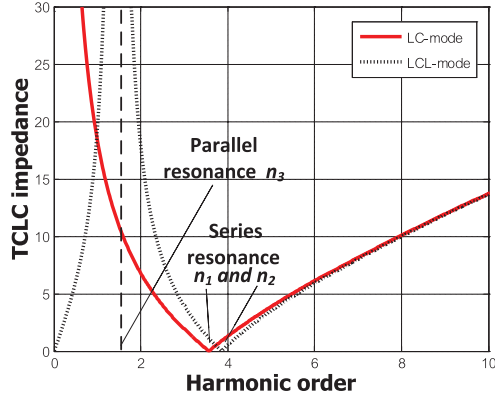


Fig. 4. TCLC impedance under different harmonic order.

Based on the above discussion, the design criteria of  $L_c$  can be expressed as

$$L_c = \frac{1}{(\omega n_1)^2 C_{PF}} \quad \text{and} \quad L_c = \frac{1}{(\omega n_2)^2 C_{PF} - 1/L_{PF}} \quad (16)$$

$$n_3 = \frac{1}{\sqrt{L_{PF} C_{PF} \omega^2}} \quad (n_1, n_2, \text{ and } n_3 \text{ away from } n_d). \quad (17)$$

In (16), they can be satisfied simultaneously as long as  $n_1$  and  $n_2$  are away from the dominated harmonic orders  $n_d$ . The designed  $C_{PF}$  and  $L_{PF}$  should also satisfy (17). In this paper,  $n_1 = 3.6, n_2 = 3.9$ , and  $n_3 = 1.5$  are chosen.

### C. Design of $V_{dc}$

Different with the traditional  $V_{dc}$  design method of the STATCOM to compensate maximum load reactive power, the  $V_{dc}$  of Hybrid-STATCOM is design to solve the firing angle mistuning problem of TCLC (i.e., affect the reactive power compensation) so that the source reactive power can be fully compensated. Reforming (3), the inverter voltage  $V_{invx}$  can also be expressed as

$$V_{invx} = V_x \left[ 1 + \frac{V_x I_{Lqx}}{V_x^2 / X_{TCLC}(\alpha_x)} \right] = V_x \left[ 1 + \frac{Q_{Lx}}{Q_{cx, TCLC}(\alpha_x)} \right] \quad (18)$$

where  $Q_{Lx}$  is the load reactive power,  $Q_{cx, TCLC}(\alpha_x)$  is the TCLC part compensating reactive power, and  $V_x$  is the RMS value of the load voltage. Combining (18) with  $V_{dc} = \sqrt{6} |V_{invx}|$ , the required dc-link voltage  $V_{dc}$  for hybrid-STATCOM can be expressed as

$$V_{dc} = \sqrt{6} V_x \left| 1 + \frac{Q_{Lx}}{Q_{cx, TCLC}(\alpha_x)} \right|. \quad (19)$$

Ideally,  $Q_{cx, TCLC}(\alpha_x)$  is controlled to be equal to  $-Q_{Lx}$  so that the required  $V_{dc}$  can be zero. However, in the practical case, the  $Q_{cx, TCLC}(\alpha_x)$  may not be exactly equal to  $-Q_{Lx}$  due to the firing angle mistuning problem. The worst case of mistuning  $Q_{Lx}/Q_{cx, TCLC}(\alpha_x)$  ratio can be premeasured to estimate the required minimum  $V_{dc}$  value. Finally, a slightly greater  $V_{dc}$  value can be chosen.

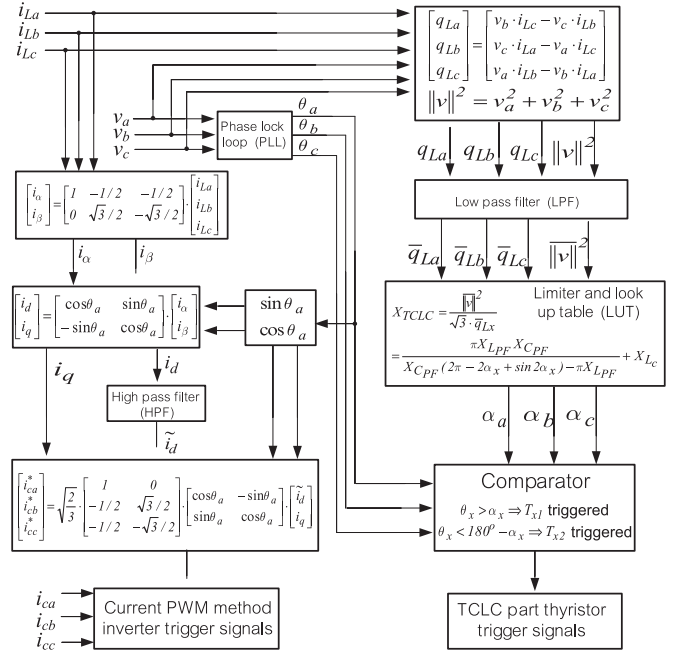


Fig. 5. Control block diagram of hybrid-STATCOM.

Based on (12), (13), (16), and (19), the system parameters  $C_{PF}$ ,  $L_{PF}$ ,  $L_c$ , and  $V_{dc}$  of hybrid-STATCOM can be designed accordingly. In the following section, the control strategy of hybrid-STATCOM is proposed and discussed.

## V. CONTROL STRATEGY OF HYBRID-STATCOM

In this section, a control strategy for hybrid-STATCOM is proposed by coordinating the control of the TCLC part and the active inverter part so that the two parts can complement each other's disadvantages, and the overall performance of hybrid-STATCOM can be improved. Specifically, with the proposed controller, the response time of hybrid-STATCOM can be faster than SVCs, and the active inverter part can operate at lower dc-link operating voltage than the traditional STATCOMs. The control strategy of hybrid-STATCOM is separated into two parts for discussion: A. TCLC part control and B. Active inverter part control. The response time of hybrid-STATCOM is discussed in part C. The control block diagram of hybrid-STATCOM is shown in Fig. 5.

### A. TCLC Part Control

Different with the traditional SVC control based on the traditional definition of reactive power [2], [3], to improve its response time, the TCLC part control is based on the instantaneous pq theory [4]. The TCLC part is mainly used to compensate the reactive current with the controllable TCLC part impedance  $X_{TCLC}$ . Referring to (3), to obtain the minimum inverter voltage  $V_{invx} \approx 0$ ,  $X_{TCLC}$  can be calculated with Ohm's law in terms of the RMS values of the load voltage ( $V_x$ ) and the load reactive current ( $I_{Lqx}$ ). However, to calculate the  $X_{TCLC}$  in real time, the expression of  $X_{TCLC}$  can be rewritten in terms of instantaneous values as

$$X_{\text{TCLC}} = \frac{V_x}{I_{Lqx}} = \frac{\|v\|^2}{\sqrt{3} \cdot \bar{q}_{Lx}} \quad (20)$$

where  $\|v\|$  is the norm of the three-phase instantaneous load voltage and  $\bar{q}_{Lx}$  is the dc component of the phase reactive power. The real-time expression of  $\|v\|$  and  $\bar{q}_{Lx}$  can be obtained by (21) and (22) with low-pass filters

$$\|v\| = \sqrt{v_a^2 + v_b^2 + v_c^2} \quad (21)$$

$$\begin{bmatrix} q_{La} \\ q_{Lb} \\ q_{Lc} \end{bmatrix} = \begin{bmatrix} v_b \cdot i_{Lc} - v_c \cdot i_{Lb} \\ v_c \cdot i_{La} - v_a \cdot i_{Lc} \\ v_a \cdot i_{Lb} - v_b \cdot i_{La} \end{bmatrix}. \quad (22)$$

In (21) and (22),  $v_x$  and  $q_{Lx}$  are the instantaneous load voltage and the load reactive power, respectively. As shown in Fig. 5, a limiter is applied to limit the calculated  $X_{\text{TCLC}}$  in (9) within the range of  $X_{\text{TCLC}} > X_{\text{ind}(\min)}$  and  $X_{\text{TCLC}} < X_{\text{Cap}(\min)}$  ( $X_{\text{Cap}(\min)} < 0$ ). With the calculated  $X_{\text{TCLC}}$ , the firing angle  $\alpha_x$  can be determined by solving (4). Because (4) is complicated, a look-up table (LUT) is installed inside the controller. The trigger signals to control the TCLC part can then be generated by comparing the firing angle  $\alpha_x$  with  $\theta_x$ , which is the phase angle of the load voltage  $v_x$ .  $\theta_x$  can be obtained by using a phase lock loop (PLL). Note that the firing angle of each phase can differ if the unbalanced loads are connected [see (4) and (20)]. With the proposed control algorithm, the reactive power of each phase can be compensated, and the active power can be basically balanced, so that dc-link voltage can be maintained at a low level even under unbalanced load compensation.

### B. Active Inverter Part Control

In the proposed control strategy, the instantaneous active and reactive current  $i_d$ - $i_q$  method [7] is implemented for the active inverter part to improve the overall performance of hybrid-STATCOM under different voltage and current conditions, such as balanced/unbalanced, voltage dip, and voltage fault. Specifically, the active inverter part is used to improve the TCLC part characteristic by limiting the compensating current  $i_{cx}$  to its reference value  $i_{cx}^*$  so that the mistuning problem, the resonance problem, and the harmonic injection problem can be avoided. The  $i_{cx}^*$  is calculated by applying the  $i_d$ - $i_q$  method [7] because it is valid for different voltage and current conditions.

The calculated  $i_{cx}^*$  contains reactive power, unbalanced power, and current harmonic components. By controlling the compensating current  $i_{cx}$  to track its reference  $i_{cx}^*$ , the active inverter part can compensate for the load harmonic currents and improve the reactive power compensation ability and dynamic performance of the TCLC part under different voltage conditions. The  $i_{cx}^*$  can be calculated as

$$\begin{bmatrix} i_{ca}^* \\ i_{cb}^* \\ i_{cc}^* \end{bmatrix} = \sqrt{\frac{2}{3}} \cdot \begin{bmatrix} 1 & 0 \\ -1/2 & \sqrt{3}/2 \\ -1/2 & -\sqrt{3}/2 \end{bmatrix} \cdot \begin{bmatrix} \cos \theta_a & -\sin \theta_a \\ \sin \theta_a & \cos \theta_a \end{bmatrix} \cdot \begin{bmatrix} \tilde{i}_d \\ \tilde{i}_q \end{bmatrix} \quad (23)$$

where  $i_d$  and  $i_q$  are the instantaneous active and reactive current, which include dc components  $\tilde{i}_d$  and  $\tilde{i}_q$ , and ac components  $\tilde{i}_d$  and  $\tilde{i}_q$ .  $\tilde{i}_d$  is obtained by passing  $i_d$  through a high-pass filter.  $i_d$  and  $i_q$  are obtained by

$$\begin{bmatrix} i_d \\ i_q \end{bmatrix} = \begin{bmatrix} \cos \theta_a & \sin \theta_a \\ -\sin \theta_a & \cos \theta_a \end{bmatrix} \cdot \begin{bmatrix} i_\alpha \\ i_\beta \end{bmatrix}. \quad (24)$$

In (24), the currents ( $i_\alpha$  and  $i_\beta$ ) in  $\alpha$ - $\beta$  plane are transformed from  $a$ - $b$ - $c$  frames by

$$\begin{bmatrix} i_\alpha \\ i_\beta \end{bmatrix} = \begin{bmatrix} 1 & -1/2 & -1/2 \\ 0 & \sqrt{3}/2 & -\sqrt{3}/2 \end{bmatrix} \cdot \begin{bmatrix} i_{La} \\ i_{Lb} \\ i_{Lc} \end{bmatrix} \quad (25)$$

where  $i_{Lx}$  is the load current signal.

### C. Response Time of Hybrid-STATCOM

The TCLC part has two back-to-back connected thyristors in each phase that are triggered alternately in every half cycle, so that the control period of the TCLC part is one cycle (0.02 s). However, the proposed hybrid-STATCOM structure connects the TCLC part in series with an instantaneous operated active inverter part, which can significantly improve its overall response time. With the proposed controller, the active inverter part can limit the compensating current  $i_{cx}$  to its reference value  $i_{cx}^*$  via pulse width modulation (PWM) control, and the PWM control frequency is set to be 12.5 kHz. During the transient state, the response time of hybrid-STATCOM can be separately discussed in the following two cases. 1) If the load reactive power is dynamically changing within the inductive range (or within the capacitive range), the response time of hybrid-STATCOM can be as fast as traditional STATCOM. 2) In contrast, when the load reactive power suddenly changes from capacitive to inductive or vice versa, the hybrid-STATCOM may take approximately one cycle to settle down. However, in practical application, case 2 described above seldom happens. Therefore, based on the above discussion, the proposed hybrid-STATCOM can be considered as a fast-response reactive power compensator in which the dynamic performances of hybrid-STATCOM are proved by the simulation result (Fig. 6) and the experimental results (Figs. 7, 8, 10, and 12).

The following section reports the simulation and experimental results to verify the above  $V$ - $I$  characteristics analysis and the control strategy of the hybrid-STATCOM in comparison with traditional STATCOM and C-STATCOM.

## VI. SIMULATION RESULTS

In this section, the simulation results among traditional STATCOM, C-STATCOM, and the proposed hybrid-STATCOM are discussed and compared. The previous discussions of the required inverter voltages (or dc-link voltage  $V_{dc} = \sqrt{2} \cdot \sqrt{3} \cdot V_{invx}$ ) for these three STATCOMs are also verified by simulations. The STATCOMs are simulated with the same voltage level as in the experimental results in Section VI. The simulation studies are carried out with PSCAD/EMTDC.

TABLE II

SIMULATION RESULTS FOR INDUCTIVE AND CAPACITIVE REACTIVE POWER COMPENSATION OF TRADITIONAL STATCOM, C-STATCOM, AND HYBRID-STATCOM

Loading Type	Without and with STATCOM comp.	$i_{sx}$ (A)	DPF	THD $_{isx}$ (%)	$V_{dc}$ (V)
Case A: inductive and light loading	Before comp.	6.50	0.83	0.01	–
	Trad. STATCOM	5.55	1.00	7.22	300
	C-STATCOM	5.48	1.00	2.01	80
	Hybrid STATCOM	5.48	1.00	1.98	50
Case B: inductive and heavy loading	Before comp.	8.40	0.69	0.01	–
	Trad. STATCOM	5.95	1.00	6.55	300
	C-STATCOM	6.30	0.85	17.5	50
	C-STATCOM	5.90	0.98	7.02	300
Case C: capacitive loading	Before comp.	4.34	0.78	0.01	–
	Trad. STATCOM	3.67	1.00	7.61	250
	C-STATCOM	7.10	0.57	23.5	50
	C-STATCOM	5.02	0.99	10.6	500
	Hybrid STATCOM	3.41	1.00	3.01	50

\*Shaded areas indicate unsatisfactory results.

Table IV shows the simulation system parameters for traditional STATCOM, C-STATCOM, and hybrid-STATCOM. In addition, three different cases of loading are built for testing: A) inductive and light loading; B) inductive and heavy loading; and C) capacitive loading. These three testing cases are also represented by points A, B, and C in Fig. 2. The detailed simulation results are summarized in Table II. Finally, the dynamic response of hybrid-STATCOM is simulated and discussed in Section VI-D. With the consideration of IEEE Standard 519-2014 [24], total demand distortion (TDD) = 15%, and  $I_{SC}/I_L$  in  $100 < 1000$  scale at a typical case, the nominal rate current is assumed to be equal to the fundamental load current in the worst-case analysis, which results in  $THD = TDD = 15\%$ . Therefore, this paper evaluates the compensation performance by setting  $THD < 15\%$ .

### A. Inductive and Light Loading

When the loading is inductive and light, traditional STATCOM requires a high dc-link voltage ( $V_{dc} > \sqrt{2} \cdot V_{L-L} = 269V$ ,  $V_{dc} = 300V$ ) for compensation. After compensation, the source current  $i_{sx}$  is reduced to 5.55 A from 6.50 A, and the source-side displacement power factor (DPF) becomes unity from 0.83. In addition, the source current total harmonics distortion (THD $_{isx}$ ) is 7.22% after compensation, which satisfies the international standard [24] (THD $_{isx} < 15\%$ ).

For C-STATCOM, the coupling impedance contributes a large voltage drop between the load voltage and the inverter voltage so that the required dc-link voltage can be small ( $V_{dc} = 80V$ ). The  $i_{sx}$ , DPF, and THD $_{isx}$  are compensated to 5.48 A, unity, and 2.01%, respectively.

For the proposed hybrid-STATCOM, the  $i_{sx}$ , DPF, and THD $_{isx}$  are compensated to 5.48 A, unity, and 1.98%, respectively. As discussed in the previous section, a low dc-link voltage ( $V_{dc} = 50V$ ) of hybrid-STATCOM is used to avoid mistuning of firing angles, prevent resonance problems, and reduce the injected harmonic currents.

### B. Inductive and Heavy Loading

To compensate for the inductive and heavy loading, traditional STATCOM still requires a high dc-link voltage of  $V_{dc} = 300V$  for compensation. Traditional STATCOM can obtain acceptable results (DPF = 1.00 and THD $_{isx} = 6.55\%$ ). The  $i_{sx}$  is reduced to 5.95 A from 8.40 A after compensation.

With a low dc-link voltage ( $V_{dc} = 50V$ ), C-STATCOM cannot provide satisfactory compensation results (DPF = 0.85 and THD $_{isx} = 17.5\%$ ). However, when the dc-link voltage is increased to  $V_{dc} = 300V$ , the compensation results (DPF = 1.00 and THD $_{isx} = 7.02\%$ ) are acceptable and satisfy the international standard [24] (THD $_{isx} < 15\%$ ). The  $i_{sx}$  is reduced to 5.90 A from 8.40 A after compensation.

On the other hand, the proposed hybrid-STATCOM can still obtain acceptable compensation results (DPF = 1.00 and THD $_{isx} = 3.01\%$ ) with a low dc-link voltage of  $V_{dc} = 50V$ . The  $i_{sx}$  is reduced to 5.89 A from 8.40 A after compensation.

### C. Capacitive Loading

When the loading is capacitive, with  $V_{dc} = 250V$  ( $V_{dc} < \sqrt{2} \cdot V_{L-L} = 269V$ ), the compensation results of traditional STATCOM are acceptable, in which the DPF and THD $_{isx}$  are compensated to unity and 7.61%. The  $i_{sx}$  is also reduced to 3.67 A from 4.34 A after compensation.

For C-STATCOM with  $V_{dc} = 50V$ , the  $i_{sx}$  increases to 7.10 A from the original 4.34 A. The compensation performances (DPF = 0.57 and THD $_{isx} = 23.5\%$ ) are not satisfactory, which cannot satisfy the international standard [24] (THD $_{isx} < 15\%$ ). When  $V_{dc}$  is increased to 500 V, the DPF is improved to 0.99, and the THD $_{isx}$  is reduced to 10.6%, which can be explained by its  $V-I$  characteristic. However, the compensated  $i_{sx} = 5.02A$  is still larger than  $i_{sx} = 3.73A$  before compensation.

With the lowest dc-link voltage ( $V_{dc} = 50V$ ) of the three STATCOMs, hybrid-STATCOM can still obtain the best compensation results with DPF = 1.00 and THD $_{isx} = 3.01\%$ . In addition, the  $i_{sx}$  is reduced to 3.41 A from 4.34 A after compensation.

### D. Dynamic Response of Hybrid-STATCOM

Fig. 6 shows the dynamic performance of hybrid-STATCOM for different loadings compensation. When the load reactive power changes from capacitive to inductive, hybrid-STATCOM takes about one cycle to settle down. However, when the load reactive power is changing within the inductive range, the transient time is significantly reduced and the waveforms are smooth. Meanwhile, the fundamental reactive power is compensated to around zero even during the transient time. In practical situations, the load reactive power seldom suddenly changes from capacitive to inductive or vice versa, and thus, hybrid-STATCOM can obtain good dynamic performance.

According to the above simulation results, Table II verifies the  $V-I$  characteristics of the traditional STATCOM, C-STATCOM, and hybrid-STATCOM, as shown in Fig. 2. With similar compensation performance, the capacity of the

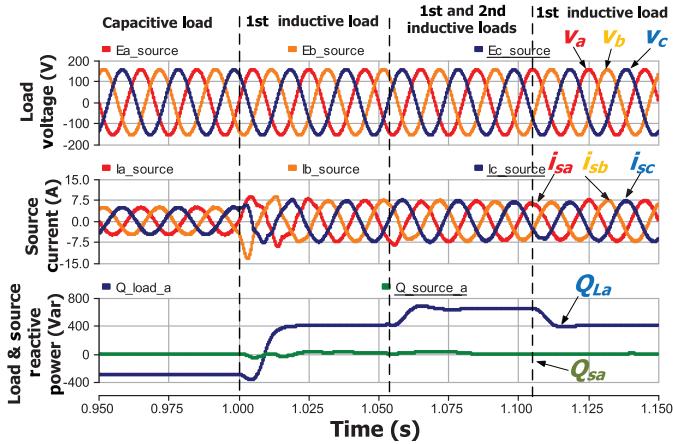


Fig. 6. Dynamic compensation waveforms of load voltage, source current, and load and source reactive powers by applying hybrid-STATCOM under different loadings cases.

active inverter part (or dc-link voltage) of the proposed hybrid-STATCOM is only about 16% of that of traditional STATCOM under wide range compensation (both inductive and capacitive). According to the cost study in [14] and [17], the average cost of traditional STATCOM is around USD 60\$/kVA, whereas that of SVC is only approximately 23\$/kVA. Therefore, by rough calculation, the average cost of the proposed hybrid-STATCOM is just about 33\$/kVA ( $= 60\$/kVA * 16\% + 23\$/kVA$ ), which is 55% of the average cost of traditional STATCOM. Moreover, because the proposed hybrid-STATCOM can avoid the use of multilevel structures in medium-voltage level transmission system in comparison to traditional STATCOM, the system reliability can be highly increased and the system control complexity and operational costs can be greatly reduced.

Based on the above simulation results, a summary can be drawn as follows.

- 1) The traditional STATCOM can compensate for both inductive and capacitive reactive currents with a high dc-link operating voltage due to a small coupling inductor.
- 2) Due to its high dc-link voltage, the traditional STATCOM obtains the poor source current THD<sub>isx</sub> (caused by switching noise) compared with hybrid-STATCOM.
- 3) C-STATCOM has a low dc-link voltage characteristic only under a narrow inductive loading range. However, when the loading current is outside its designed range, the C-STATCOM requires a very high dc-link operating voltage due to a large coupling capacitor.
- 4) The hybrid-STATCOM obtains the best performances of the three STATCOMs under both inductive and capacitive loadings.
- 5) The hybrid-STATCOM has a wide compensation range with low dc-link voltage characteristic and good dynamic performance.

## VII. EXPERIMENTAL RESULTS

The objective of the experiment results is to verify that the proposed hybrid-STATCOM has the characteristics of a wide compensation range and low dc-link voltage under different

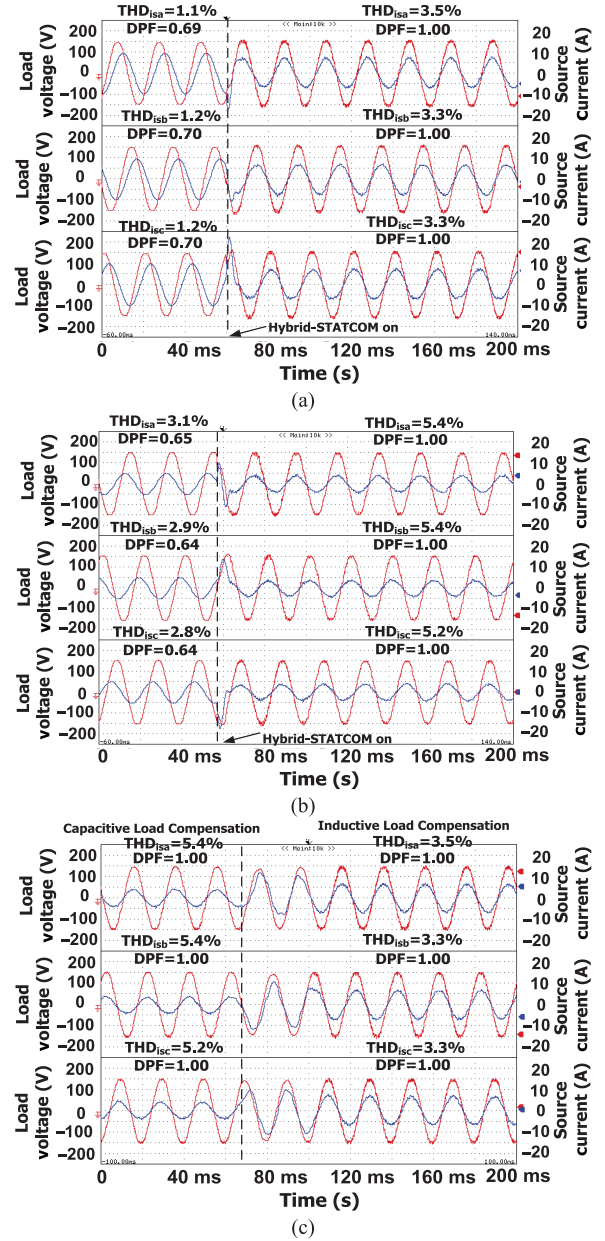


Fig. 7. Dynamic compensation waveforms of  $v_x$  and  $i_{sx}$  by applying hybrid-STATCOM under (a) inductive load; (b) capacitive load; and (c) changing from capacitive load to inductive load.

voltage and current conditions, such as unbalanced current, voltage dip, and voltage fault. The detailed settings of a 110-V, 5-kVA hybrid-STATCOM experimental system are provided in Appendix, and its dc-link voltage is maintained at  $V_{dc} = 50$  V for all experiments.

Figs. 7 and 8 show the dynamic compensation waveforms of load voltage  $v_x$ , source current  $i_{sx}$ , and reactive power  $Q_{sa}$  of phase  $a$  by applying hybrid-STATCOM for inductive load and capacitive load compensation. Fig. 9 gives the corresponding source current harmonic spectrums for inductive and capacitive reactive power compensations.

Fig. 7 clearly shows that after hybrid-STATCOM compensation, the source current  $i_{sx}$  and the load voltage  $v_x$  are in phase with each other. The source DPFs are compensated to 1.00 from

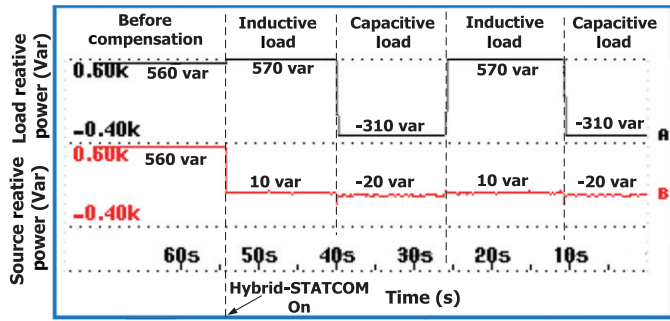


Fig. 8. Dynamic reactive power compensation of phase a by applying hybrid-STATCOM.

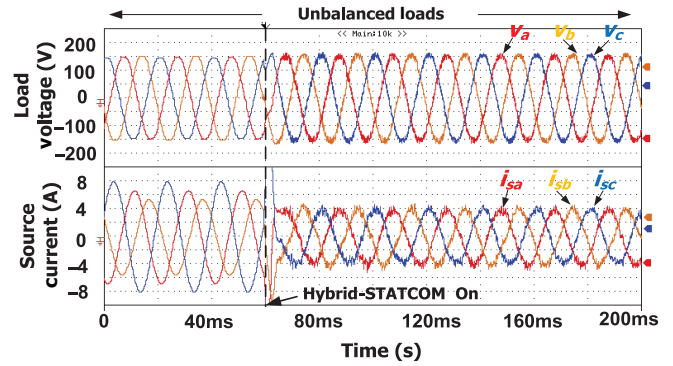


Fig. 10. Dynamic compensation waveforms of  $v_x$  and  $i_{sx}$  by applying hybrid-STATCOM under unbalanced loads.

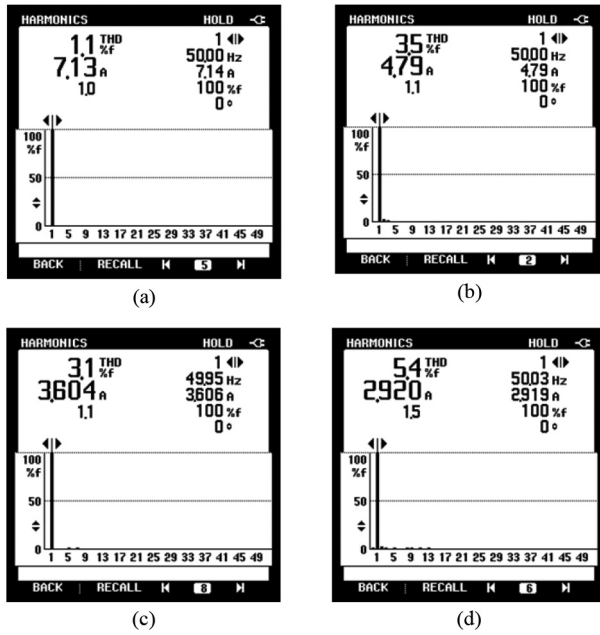


Fig. 9. Source current harmonic spectra of phase a: (a) before compensation of inductive load; (b) after compensation of inductive load; (c) before compensation of capacitive load; and (d) after compensation of capacitive load.

the original 0.69 (for inductive loading) and 0.64 (for capacitive loading). The worst phase source currents THD  $i_{sx}$  are 3.5% and 5.4% after compensation, which satisfy the international standard [24] ( $THD_{i_{sx}} < 15\%$ ). The source currents  $i_{sx}$  are also significantly reduced after compensation. In Fig. 7(a) and (b), the hybrid-STATCOM obtains a good dynamic compensation performance. In Fig. 7(c), the response time is longer than expected by one cycle because the inductive loads and capacitive loads are manually switching on and off.

Figs. 10 and 12 illustrate dynamic compensation waveforms of load voltage  $v_x$  and source current  $i_{sx}$  by applying hybrid-STATCOM under unbalanced loads and voltage fault situations, which clearly verify its good dynamic performance. Figs. 11 and 13 give their corresponding source current harmonic spectrums.

Figs. 10 and 11 show that the proposed hybrid-STATCOM can compensate for and balance the source current even under unbalanced loads with low  $V_{dc} = 50$  V. The unbalanced  $i_{sx}$  are compensated from 4.80, 3.83, and 5.74 A to 2.94, 2.79, and

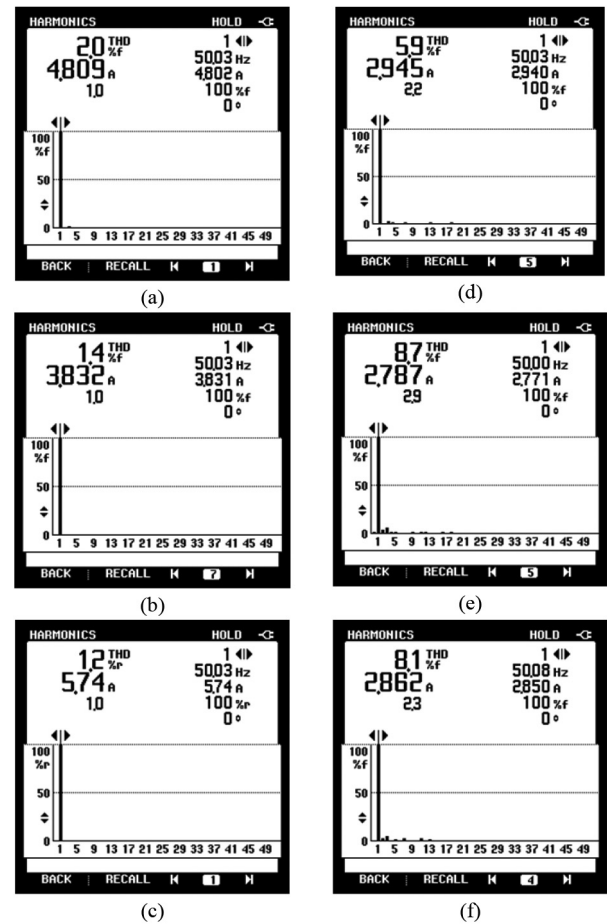


Fig. 11. Source current harmonic spectrums under unbalanced loads before compensation: (a) phase a; (b) phase b; and (c) phase c, and after hybrid-STATCOM compensation: (d) phase a; (e) phase b; and (f) phase c.

2.86 A, respectively. The DPF and  $THD_{i_{sx}}$  are compensated to unity and lower than 9.0%, which satisfy the international standard [24]. From Figs. 12 and 13, it can be seen that the proposed hybrid-STATCOM can still obtain satisfactory performances even under asymmetric grid fault. During the voltage fault, the  $i_{sx}$  can be compensated to be approximately balanced with  $DPF \approx 1$  and  $THD_{i_{sx}} < 10.0\%$ .

Fig. 14 also provides the dynamic compensation waveforms of load voltage  $v_x$  and source current  $i_{sx}$  by applying

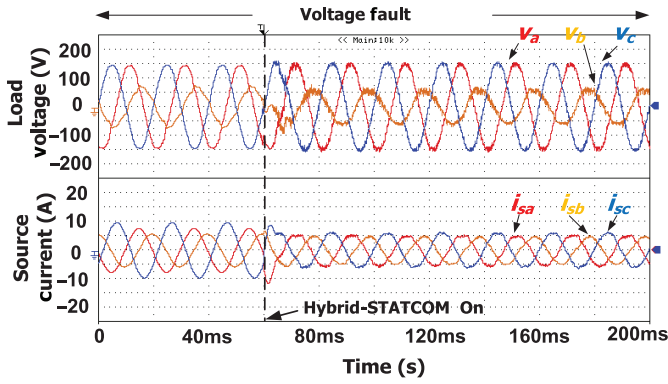


Fig. 12. Dynamic compensation waveforms of  $v_x$  and  $i_{sx}$  by applying hybrid-STATCOM under voltage fault condition.

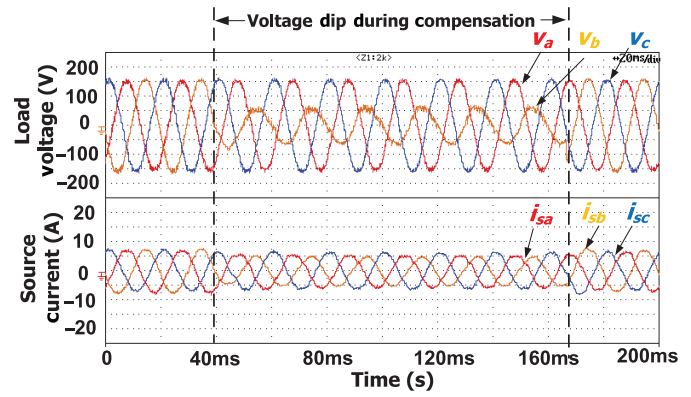


Fig. 14. Dynamic compensation waveforms of  $v_x$  and  $i_{sx}$  by applying hybrid-STATCOM during voltage dip.

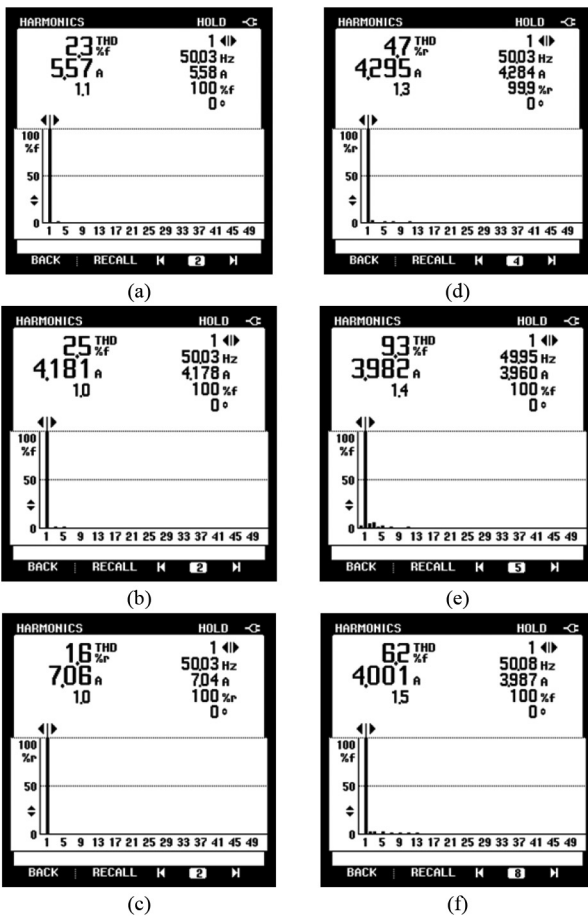


Fig. 13. Source current harmonic spectrum under voltage fault before compensation: (a) phase a; (b) phase b; and (c) phase c, and after hybrid-STATCOM compensation: (d) phase a; (e) phase b; and (f) phase c.

hybrid-STATCOM during a sudden voltage dip. It is found that hybrid-STATCOM can obtain good dynamic and reactive power compensation performances.

Table III summarizes the hybrid-STATCOM experimental results. The above experimental results confirm that the hybrid-STATCOM has a wide reactive power compensation range and low dc-link voltage characteristics with good dynamic performance even under different voltage and current conditions.

TABLE III

EXPERIMENTAL COMPENSATION RESULTS BY HYBRID-STATCOM ( $V_{dc} = 50$  V) UNDER DIFFERENT SYSTEM AND LOADING SITUATIONS

Different situations	Comp.	$i_{sx}$ (A)			DPF			THD $i_{sx}$ (%)		
		A	B	C	A	B	C	A	B	C
Inductive load	Before	7.13	7.14	7.34	0.69	0.70	0.70	1.1	1.2	1.2
	After	4.79	4.97	4.95	1.00	1.00	1.00	3.5	3.3	3.3
Capacitive load	Before	3.60	3.63	3.65	0.65	0.64	0.64	3.1	2.9	2.8
	After	2.92	2.80	2.85	1.00	1.00	1.00	5.4	5.4	5.2
Unbalanced loads	Before	4.80	3.83	5.74	0.36	0.69	0.64	2.0	1.4	1.2
	After	2.94	2.79	2.86	1.00	1.00	1.00	5.9	8.7	8.1
Voltage fault	Before	5.57	4.18	7.06	0.67	0.38	0.87	2.3	2.5	1.6
	After	4.30	3.98	4.00	0.99	1.00	0.99	4.7	9.3	6.2

### VIII. CONCLUSION

In this paper, a hybrid-STATCOM in three-phase power system has been proposed and discussed as a cost-effective reactive power compensator for medium voltage level application. The system configuration and  $V-I$  characteristic of the hybrid-STATCOM were analyzed, discussed, and compared with traditional STATCOM and C-STATCOM. In addition, its parameter design method was proposed on the basis of consideration of the reactive power compensation range and prevention of a potential resonance problem. Moreover, the control strategy of the hybrid-STATCOM was developed under different voltage and current conditions. Finally, the wide compensation range and low dc-link voltage characteristics with good dynamic performance of the hybrid-STATCOM were proved by both simulation and experimental results.

### APPENDIX

#### SETTINGS OF SIMULATIONS AND EXPERIMENTS

Table IV shows the simulation system parameters for traditional STATCOM, C-STATCOM, and hybrid-STATCOM under different testing loads. For experimental purposes, a 110-V, 5-kVA experimental prototype of the three-phase hybrid-STATCOM is constructed in the laboratory. The control system has a sampling frequency of 25 kHz. The switching devices for the active inverter are Mitsubishi IGBTs PM300DSA060. The switching devices for the TCLC are thyristors SanRex PK110FG160. Moreover, the experimental parameters of the hybrid-STATCOM are the same as those for the simulation listed in Table IV.

TABLE IV

SIMULATION AND EXPERIMENTAL PARAMETERS FOR TRADITIONAL STATCOM, C-STATCOM, AND HYBRID-STATCOM

	Parameters	Physical values
System parameters	$v_{x}, f, L_s$	110 V, 50 Hz, 0.1 mH
Traditional STATCOM	$L$	5 mH
C-STATCOM	$L, C$	5 mH, 80 $\mu$ F
Hybrid-STATCOM	$L_c, L_{PF}, C_{PF}$	5 mH, 30 mH, 160 $\mu$ F
Case A: inductive and light loading	$L_{L1}, R_{L1}$	30 mH, 14 $\Omega$
Case B: inductive and heavy loading	$L_{L2}, R_{L2}$	30 mH, 9 $\Omega$
Case C: capacitive loading	$C_{L3}, R_{L3}$	200 $\mu$ F, 20 $\Omega$

## REFERENCES

- [1] J. Dixon, L. Moran, J. Rodriguez, and R. Domke, "Reactive power compensation technologies: State-of-the-art review," *Proc. IEEE*, vol. 93, no. 12, pp. 2144–2164, Dec. 2005.
- [2] L. Gyugyi, R. A. Otto, and T. H. Putman, "Principles and applications of static thyristor-controlled shunt compensators," *IEEE Trans. Power App. Syst.*, vol. PAS-97, no. 5, pp. 1935–1945, Sep./Oct. 1978.
- [3] T. J. Dionise, "Assessing the performance of a static VAR compensator for an electric arc furnace," *IEEE Trans. Ind. Appl.*, vol. 50, no. 3, pp. 1619–1629, May/Jun. 2014.
- [4] F. Z. Peng and J. S. Lai, "Generalized instantaneous reactive power theory for three-phase power systems," *IEEE Trans. Instrum. Meas.*, vol. 45, no. 1, pp. 293–297, Feb. 1996.
- [5] L. K. Haw, M. S. Dahidah, and H. A. F. Almurib, "A new reactive current reference algorithm for the STATCOM system based on cascaded multilevel inverters," *IEEE Trans. Power Electron.*, vol. 30, no. 7, pp. 3577–3588, Jul. 2015.
- [6] J. A. Munoz, J. R. Espinoza, C. R. Baier, L. A. Moran, J. I. Guzman, and V. M. Cardenas, "Decoupled and modular harmonic compensation for multilevel STATCOMs," *IEEE Trans. Ind. Electron.*, vol. 61, no. 6, pp. 2743–2753, Jun. 2014.
- [7] V. Soares and P. Verdelho, "An instantaneous active and reactive current component method for active filters," *IEEE Trans. Power Electron.*, vol. 15, no. 4, pp. 660–669, Jul. 2000.
- [8] M. Hagiwara, R. Maeda, and H. Akagi, "Negative-sequence reactive-power control by a PWM STATCOM based on a modular multilevel cascade converter (MMCC-SDBC)," *IEEE Trans. Ind. Appl.*, vol. 48, no. 2, pp. 720–729, Mar./Apr. 2012.
- [9] B. Singh and S. R. Arya, "Back-propagation control algorithm for power quality improvement using DSTATCOM," *IEEE Trans. Ind. Electron.*, vol. 61, no. 3, pp. 1204–1212, Mar. 2014.
- [10] M.-C. Wong, C.-S. Lam, and N.-Y. Dai, "Capacitive-coupling STATCOM and its control," Chinese Patent 200710196710.6, May 2011.
- [11] C.-S. Lam, M.-C. Wong, W.-H. Choi, X.-X. Cui, H.-M. Mei, and J.-Z. Liu, "Design and performance of an adaptive low-dc-voltage-controlled LC-Hybrid active power filter with a neutral inductor in three-phase four-wire power systems," *IEEE Trans. Ind. Electron.*, vol. 61, no. 6, pp. 2635–2647, Jun. 2014.
- [12] S. Rahmani, A. Hamadi, N. Mendalek, and K. Al-Haddad, "A new control technique for three-phase shunt hybrid power filter," *IEEE Trans. Ind. Electron.*, vol. 56, no. 8, pp. 2904–2915, Aug. 2009.
- [13] S. Rahmani, A. Hamadi, and K. Al-Haddad, "A Lyapunov-function-based control for a three-phase shunt hybrid active filter," *IEEE Trans. Ind. Electron.*, vol. 59, no. 3, pp. 1418–1429, Mar. 2012.
- [14] H. Akagi and K. Isozaki, "A hybrid active filter for a three-phase 12-pulse diode rectifier used as the front end of a medium-voltage motor drive," *IEEE Trans. Power Electron.*, vol. 27, no. 1, pp. 69–77, Jan. 2012.
- [15] C. Kumar and M. Mishra, "An improved hybrid DSATCOM topology to compensate reactive and nonlinear loads," *IEEE Trans. Ind. Electron.*, vol. 61, no. 12, pp. 6517–6527, Dec. 2014.
- [16] J. He, Y. W. Li, and F. Blaabjerg, "Flexible microgrid power quality enhancement using adaptive hybrid voltage and current controller," *IEEE Trans. Ind. Electron.*, vol. 61, no. 6, pp. 2784–2794, Jun. 2014.
- [17] S. Hu, Z. Zhang, Y. Chen *et al.*, "A new integrated hybrid power quality control system for electrical railway," *IEEE Trans. Ind. Electron.*, vol. 62, no. 10, pp. 6222–6232, Oct. 2015.
- [18] K.-W. Lao, M.-C. Wong, N. Y. Dai, C.-K. Wong, and C.-S. Lam, "A systematic approach to hybrid railway power conditioner design with harmonic compensation," *IEEE Trans. Ind. Electron.*, vol. 62, no. 2, pp. 930–942, Feb. 2015.

- [19] K.-W. Lao, N. Dai, W.-G. Liu, and M.-C. Wong, "Hybrid power quality compensator with minimum dc operation voltage design for high-speed traction power systems," *IEEE Trans. Power Electron.*, vol. 28, no. 4, pp. 2024–2036, Apr. 2013.
- [20] A. Varschavsky, J. Dixon, M. Rotella, and L. Moran, "Cascaded nine-level inverter for hybrid-series active power filter, using industrial controller," *IEEE Trans. Ind. Electron.*, vol. 57, no. 8, pp. 2761–2767, Aug. 2010.
- [21] S. P. Litran and P. Salmeron, "Reference voltage optimization of a hybrid filter for nonlinear load reference," *IEEE Trans. Ind. Electron.*, vol. 61, no. 6, pp. 2648–2654, Jun. 2014.
- [22] J. Dixon, Y. del Valle, M. Orchard, M. Ortuzar, L. Moran, and C. Maffrand, "A full compensating system for general loads, based on a combination of thyristor binary compensator, and a PWM-IGBT active power filter," *IEEE Trans. Ind. Electron.*, vol. 50, no. 5, pp. 982–989, Oct. 2003.
- [23] W. Y. Dong, "Research on control of comprehensive compensation for traction substations based on the STATCOM technology," Ph.D. dissertation, Dept. Elect. Eng., Tsinghua Univ., Beijing, China, 2009.
- [24] *IEEE Recommended Practices and Requirements for Harmonic Control in Electrical Power Systems*, IEEE Standard 519–2014, 2014.



**Lei Wang** received the B.Sc. degree in electrical and electronics engineering from the University of Macau (UM), Macau, China, in 2011, and the M.Sc. degree in electronics engineering from Hong Kong University of Science and Technology (HKUST), Hong Kong, in 2012. He has been working toward the Ph.D. degree in electrical and computer engineering at UM since 2012.

In 2012, he joined the Power Electronics Laboratory, UM. His research interests include power electronics, power quality and distribution flexible ac transmission systems (DFACTS), power quality compensation, and renewable energy. Mr. Wang was the recipient of the Champion Award in the "Schneider Electric Energy Efficiency Cup," Hong Kong, in 2011.



**Chi-Seng Lam** (S'04–M'12–SM'16) received the B.Sc., M.Sc., and Ph.D. degrees in electrical and electronics engineering from the University of Macau (UM), Macau, China, in 2003, 2006, and 2012, respectively.

From 2006 to 2009, he was an E&M Engineer with UM. From 2009 to 2012, he was a Laboratory Technician with UM. In 2013, he was a Postdoctoral Fellow with Hong Kong Polytechnic University, Hung Hom, Hong Kong. He is currently an Assistant Professor with the State Key Laboratory of Analog and Mixed Signal VLSI, UM. He has coauthored one book: *Design and Control of Hybrid Active Power Filters* (Springer, 2014) and over 50 technical journal and conference papers. His research interests include integrated controllers, power management integrated circuits, and power quality compensators.

Dr. Lam is a Secretary of the IEEE Macao Section and PES/PELS Joint Chapter. He was the recipient of the Macao Science and Technology Invention Award (Third-Class) and R&D Award for Ph.D. in 2014 and 2012, respectively, and RIUPEEEC Merit Paper Award in 2005.



**Man-Chung Wong** (SM'06) received the B.Sc. and M.Sc. degrees in electrical and electronics engineering from the University of Macau, Macau, China, in 1993 and 1997, respectively, and the Ph.D. degree in electrical engineering from Tsinghua University, Beijing, China, in 2003.

From July 2014 to December 2014, he was a Visiting Fellow at the University of Cambridge, Cambridge, U.K. He is currently an Associate Professor with the Department of Electrical and

Computer Engineering, University of Macau. He has authored more than 100 journal and conference papers.

Dr. Wong was the recipient of the Young Scientist Award from the "Instituto Internacional De Macau" in 2000, the Young Scholar Award from the University of Macau in 2001, second prize of the Tsinghua University Excellent Doctor Thesis Award in 2003, and third prize awards of the Invention Award of the Macau Government Science and Development Award in 2012 and 2014.